Supplementary Information

For

The influences of the structure of thiophene-based conjugated microporous polymers on the fluorescence sensing properties

Tong-Mou Geng*, Chen Hu, Min Liu, Can Zhang, Heng Xu, and Xie Wang

AnHui Province Key Laboratory of Optoelectronic and Magnetism Functional Materials; School of Chemistry and Chemical Engineering, Anqing Normal University, Anqing 246011, China

Corresponding Author:

Tongmou Geng

Mailing Address: School of Chemistry and Chemical Engineering, Anqing Normal University, Anqing 246011, China

Telephone: +86-0556-5500090

Fax: +86-0556-5500090

E-mail addresses: gengtongmou@aqnu.edu.cn (TM Geng).

S1. Experimental Section

S1.1. Materials

Tetrakis-(triphenylphosphine) palladium (0) ($Pd(PPh_3)_4$), cupric iodide were obtained from J&K Scientific. 2,3,4,5-tetraphenylthiophene (TPTh), 1,3,5-triethynylbenzene (TEB), 1,4-diethynylbenzene (DEB), 2,3,4,5-tetrabromothiophene (TBrTh), diisopropylamine (DIPA), dimethylformamide (DMF), dichloromethane were purchased from Aladdin. All chemicals were used without any purified.

S1.2 Synthesis of 2,5-bis(4-bromophenyl)-3,4-diphenylthiophene (BBDTh)

Admixture of Br_2 (7.06 mmol, 1.13 g) and CH_2Cl_2 (15 mL) was dropwise added into a mixture of 2,3,4,5-tetraphenylthiophene (3.53 mmol, 1.3715 g) and CH_2Cl_2 (20 mL). The dropwise addition process lasts for 15 min., and the solution is brown-red, and stirred at room temperature for 16 hours. After 16 hours, the mixture was poured into 40 mL of absolute ethyl alcohol and a large amount of yellow precipitate was produced. The suction was then carried out and washed twice with methanol and finally dried under vacuum at 50 ^oC for 10 h. Yield was 83.6%. FT-IR (cm^{-1}): 3343, 1636, 1477, 1390, 1072, 931, 701. ^1H NMR (400 MHz, $CDCl_3$) δ (ppm): 7.22, 7.32, 7.37, 7.48, 7.49. Elemental analysis of BBDTh: Calculated value (%): C 61.56, H 3.22, S 5.87; Found (%): C 61.06, H 3.153, S 5.748.

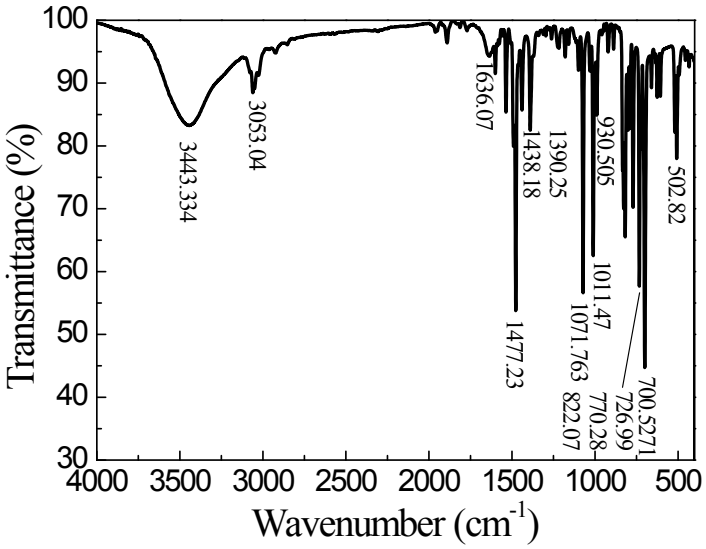

Fig. S1. FTIR spctrum of BBDTh.

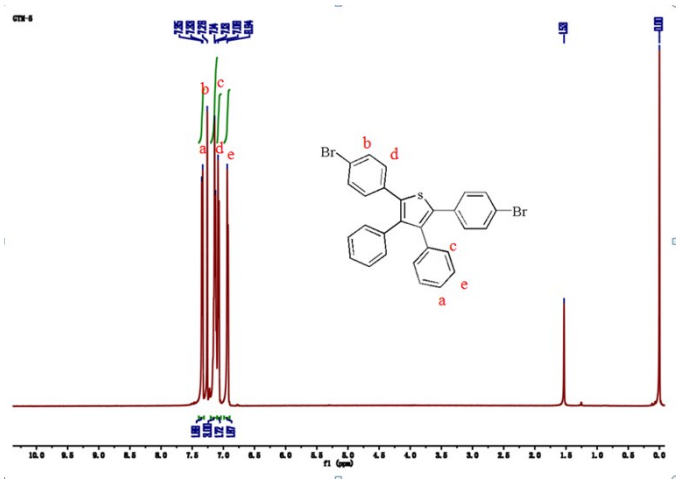

Fig. S2. ^{1}H NMR spectra of BBDTh ($DCCl_3$).

S1.2. Synthesis of the CMPs

TTPTh: A mixture of 2,5-bis(4-bromophenyl)-3,4-diphenylthiophene (BBDTh) (2.0 mmol, 1.0930 g), 1,3,5-triethynylphenyl (2.0 mmol, 0.3006 g), tetrakis-(triphenylphosphine) palladium (0) ($Pd(PPh_3)_4$) (20 mg), CuI (20 mg), (12.4 mL), and DIPA (12.4 mL) react in nitrogen in an atmosphere of 100 ^{o}C. The solution is brown red. Three days later, the reaction stopped. After cooling at room temperature, the solid was washed three times with methanol (10 mL) and chloroform (10 mL) for

each, then the product was extracted with methanol, chloroform and acetone for 24 hours using a Soxhlet extractor, respectively. The solid was dried at 50 ^{o}C in a vacuum oven for 24 h to afford brown powder (Yield was 62.72 %). FT-IR (cm^{-1}): 3442, 1636, 1384, 698. ss ^{13}C NMR (400 MHz) δ (ppm): 135.97, 130.33, 127.55, 90.19, 82.00, 76.96. Elemental analysis of TTPTh: Calculated value (%): C 88.98, H 4.22, S 6.60; Found (%): C 87.50, H 4.465, S 6.895.

DBTh: This polymer was synthesized using the similar procedures as described for TTPTh. 2,3,4,5-tetrabromothiophene (1.0 mmol, 0.3997 g), 1,3,5-triethynylbenzene (TEB) (3 mmol, 0.3784 g), tetrakis-(triphenylphosphine) palladium(0) ($Pd(PPh_3)_4$) (40 mg), CuI (20 mg), DMF (8 mL), and DIPA (8 mL) were used. DBTh was obtained as a brown powder (0.5157 g, yield: 81.57 %) IR (KBr, ν; cm^{-1}): 3445, 2202, 1657, 1504, 1461, 1396, 834, and 545. ss ^{13}C NMR (400 MHz) δ (ppm): 130.77, 122.08, 98.80, 82.87, 76.96. Elemental analysis of DBTh: Calculated value (%): C 86.72, H 3.64, S 9.65; Found (%): C 84.32, H 4.916, S 9.764.

TBTh: This polymer was synthesized using the similar procedures as described for TTPTh. 2,3,4,5-tetrabromothiophene (1.0 mmol, 0.3997 g), 1,3,5-triethynylbenzene (TEB) (2 mmol, 0.3004 g), tetrakis-(triphenylphosphine) palladium(0) ($Pd(PPh_3)_4$) (40 mg), CuI (20 mg), DMF (8 mL), and DIPA (8 mL) were used. TBTh was obtained as abrown powder (0.5012 g, yield: 73.15 %). IR (KBr, ν; cm^{-1}): 3429, 3298, 2198, 1646, 1576, 1412, 1308, 822, and 632. ss ^{13}C NMR (400 MHz) δ (ppm): 132.60, 122.26, 96.11, 80.56. Elemental analysis of TBTh: Calculated value (%): C 85.69, H 2.88, S 11.44; Found (%): C 83.34, H 2.934, S 11.726.

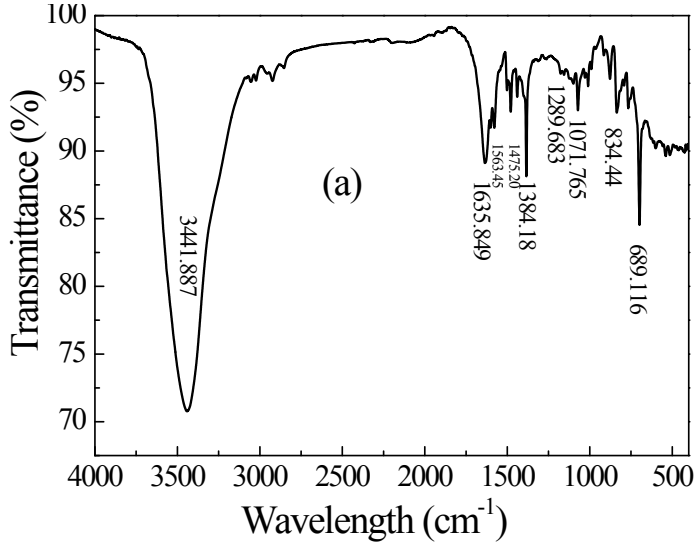
(a)
Transmittance (%)
Wavelength (cm-1)
3441.887
1635.849
1563.45
1475.20
1384.18
1289.683
1071.765
834.44
689.116

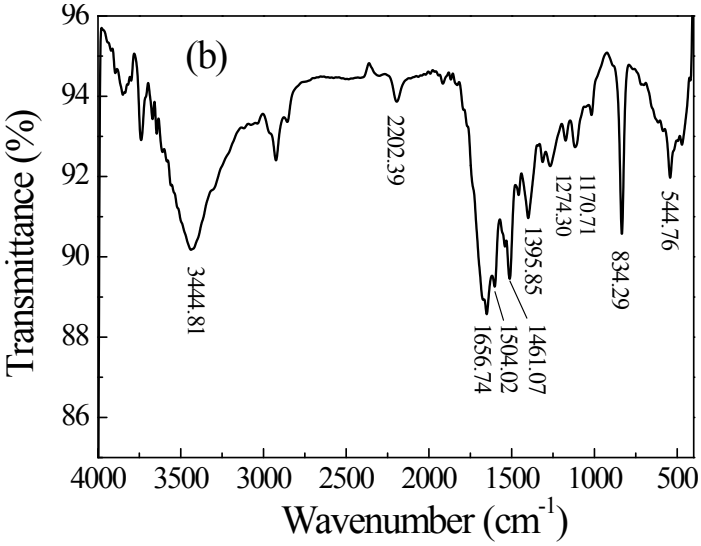
(b)
Transmittance (%)
Wavenumber (cm-1)
3444.81
2202.39
1656.74
1504.02
1461.07
1395.85
1274.30
1170.71
834.29
544.76

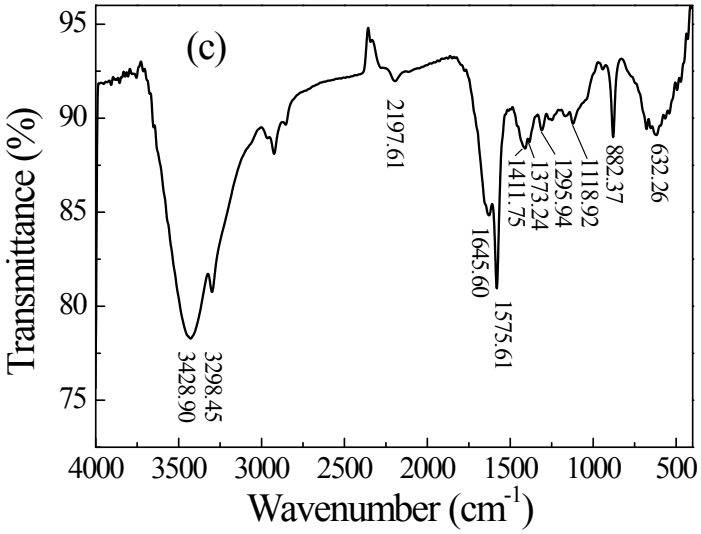
(c)
Transmittance (%)
Wavenumber (cm-1)
3428.90
3298.45
2197.61
1645.60
1575.61
1411.75
1373.24
1295.94
1118.92
882.37
632.26

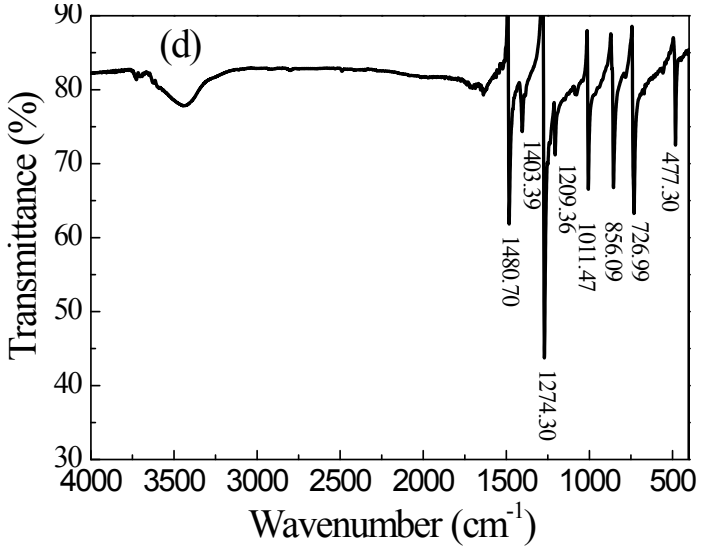

Fig. S3. FT-IR spectra of CMPs and monomer. (a) TTPTh, (b) DBTh, (c) TBTh, and (d) TBrTh.

S1. 3. Methods

Infrared spectra were recorded on an iS50 FT-IR spectrometer (400 to 4000 cm^{-1}) by using KBr pellets. Solid-state ^{13}C CP/MAS NMR measurements were recorded on a Bruker AVANCE III 400 WB spectrometer at a MAS rate of 5 kHz and a CPcontact time of 2 ms. UV−Vis spectra were recorded on an UV-2501PC spectrometer. Elemental analyses were carried out on a VARIO ELIII cube analyzer. Scanning electron microscopy was performed on a S-3400N microscope. Thermogravimetric analysis (TGA) measurements were performed on a CDR-4P TGA under N_2, by heating to 800 °C at a rate of 10 °C min^{-1}. X-ray diffraction (XRD) data were recorded on a XRD 600 diffractometer by depositing powder on glass substrate, from 2θ =5° to 90° with 0.02° increment. The Brunauer-Emmett-Teller (BET) method was utilized to calculate specific surface area and pore volume, the Saito-Foley (SF) method was applied for estimation of pore size distribution. Fluorescence spectra were recorded at room temperature using a Hitachi F-4500 spectrophotometer.

Samples were prepared as follows: dried CMPs powder (10 mg) ground with an agate mortar was added to 10 mL of organic solvents. After the resulting mixture was well dispersed with ultrasound, the dispersion colloid was obtained.

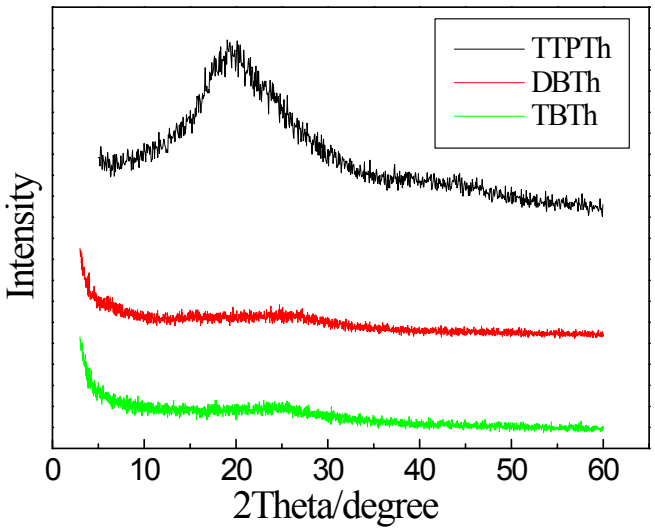

Fig. S4. PXRD patterns of TTPTh, DBTh, and TBTh.

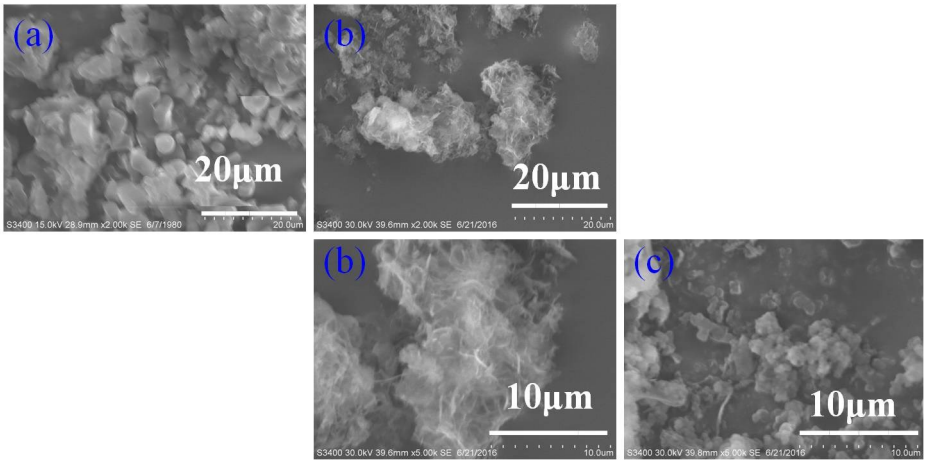

Fig. S5. The SEM images of (a) TTPTh, (b) DBTh, and (c) TBTh.

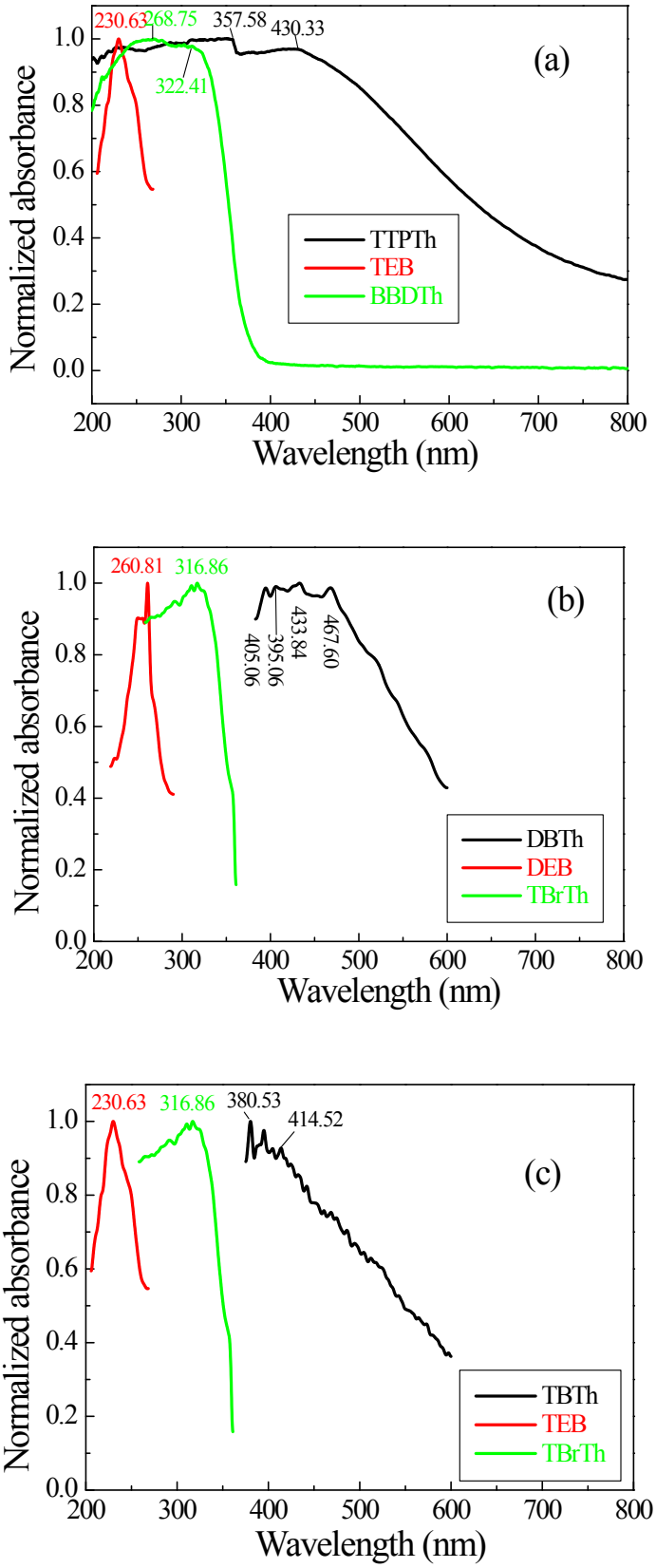

Fig. S6. UV-Vis spectra of CMPs and the corresponding monomers: (a) TTPTh, (b) DBTh, and (c) TBTh.

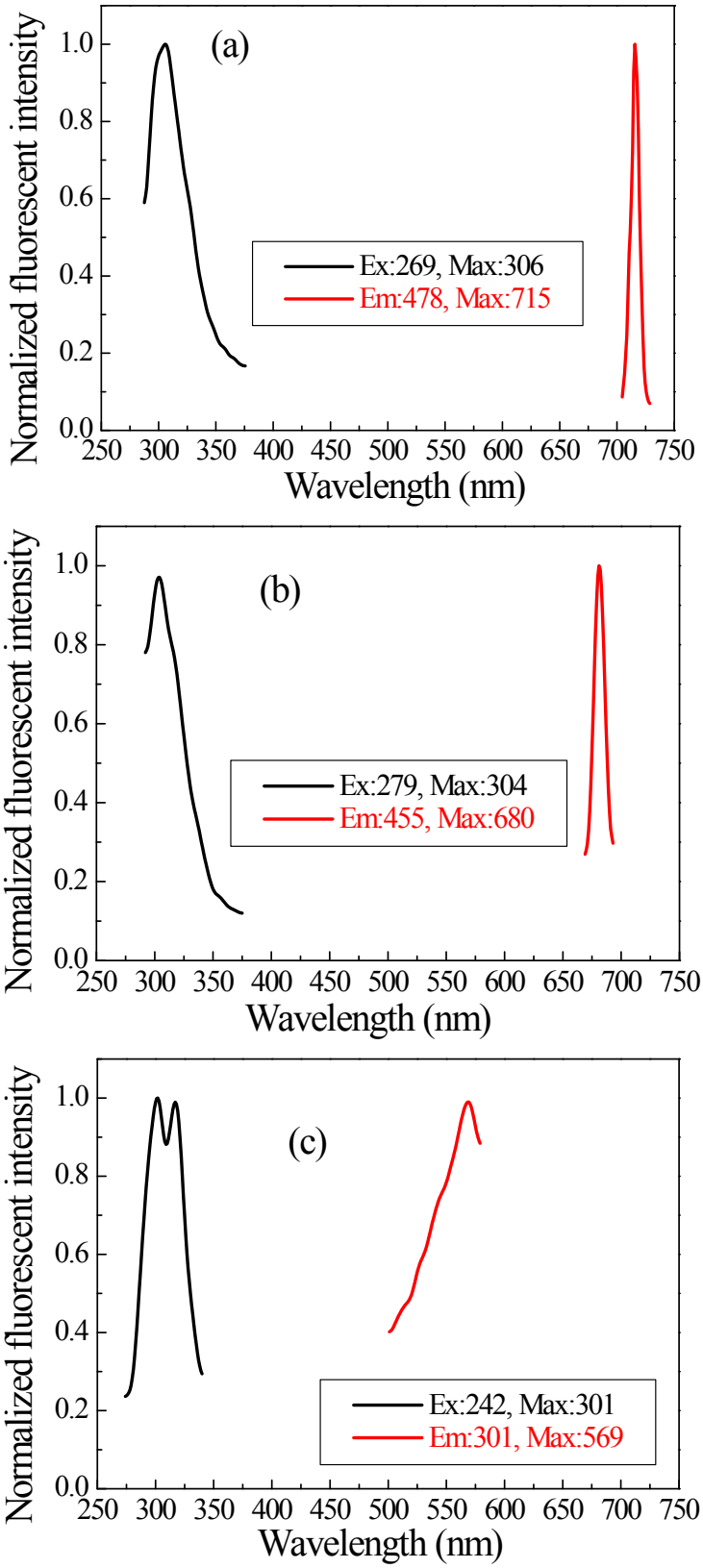

Fig. S7. The excitation (black line) and fluorescence spectra (red line) of three solid CMPs: (a) TTPTh, (b) DBTh, and (c) TBTh.

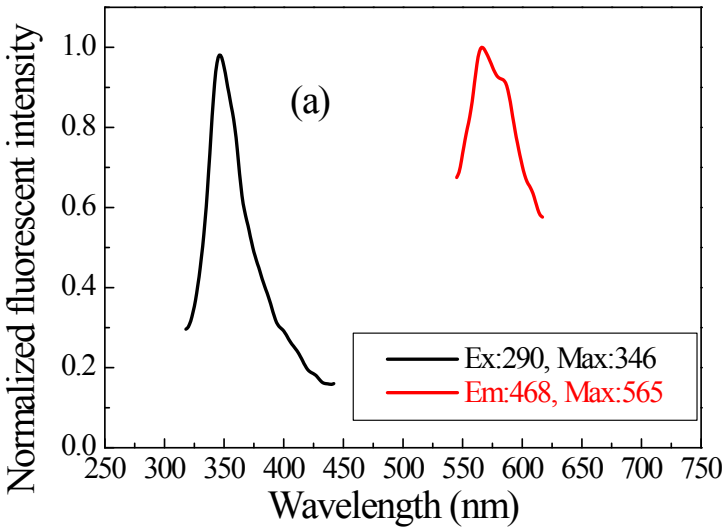
Normalized fluorescent intensity
1.0
0.8
0.6
0.4
0.2
0.0
(a)
Ex:290, Max:346
Em:468, Max:565
250 300 350 400 450 500 550 600 650 700 750
Wavelength (nm)

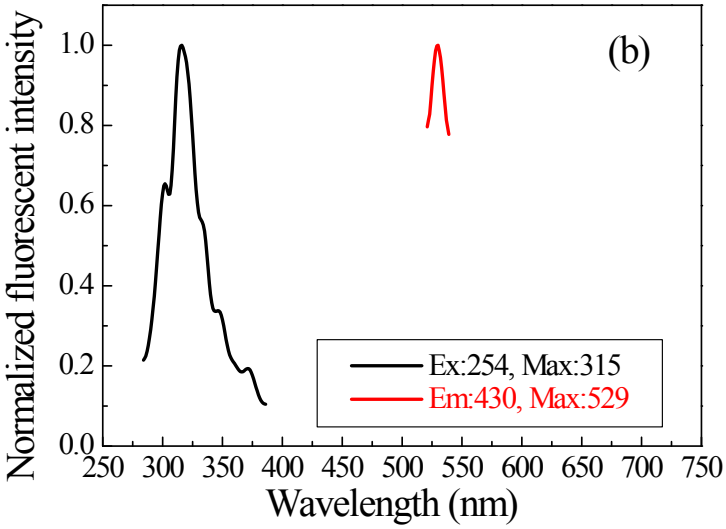
Normalized fluorescent intensity
1.0
0.8
0.6
0.4
0.2
0.0
(b)
Ex:254, Max:315
Em:430, Max:529
250 300 350 400 450 500 550 600 650 700 750
Wavelength (nm)

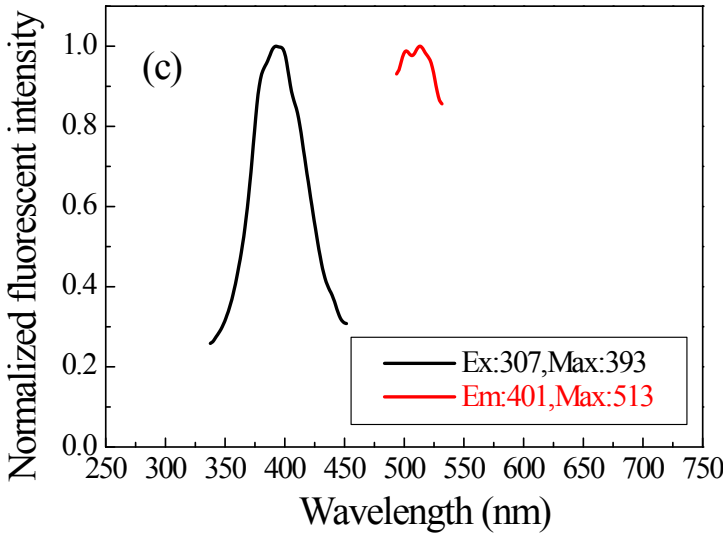
Normalized fluorescent intensity
1.0
0.8
0.6
0.4
0.2
0.0
(c)
Ex:307,Max:393
Em:401,Max:513
250 300 350 400 450 500 550 600 650 700 750
Wavelength (nm)

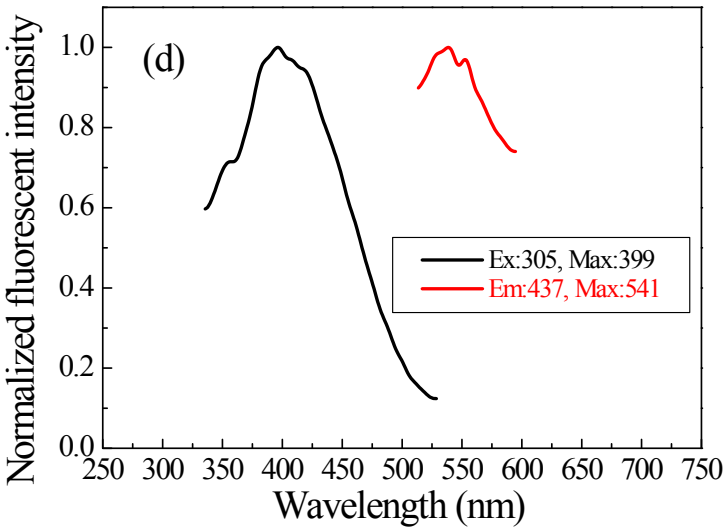

Fig. S8. The excitation (black line) and fluorescence spectra (red line) of solid monomers (a) TEB, (b) DEB, (c) BBDTh, as well as (d) model compound tetraphenylthiophene (TPTh).

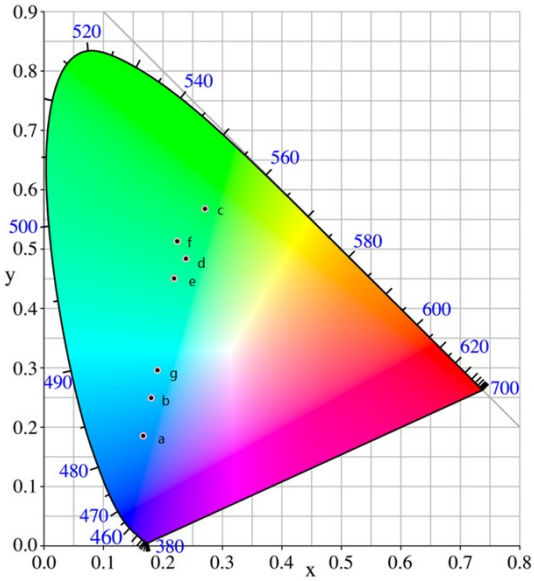

Fig. S9. CIE chromaticity diagram of DBTh under ambient condition in various solvents: a) ACN, b) Acetone, c) DMF, d) DOX, e) Chloroform, f) THF, and g) EtOH (λex=410 nm).

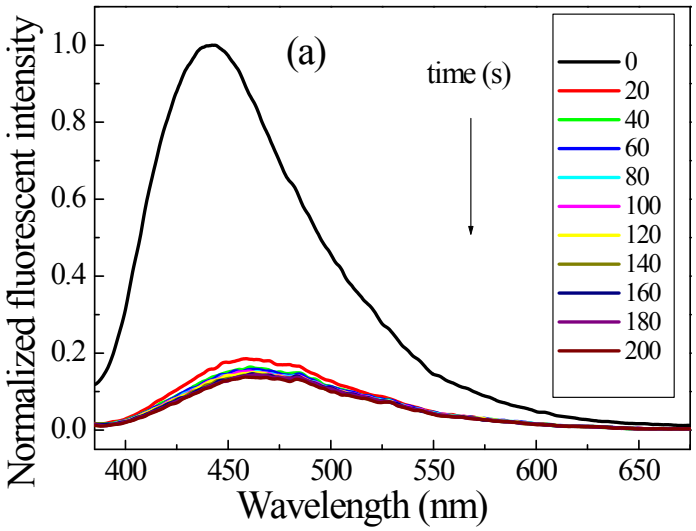
(a)
time (s)
0
20
40
60
80
100
120
140
160
180
200
Normalized fluorescent intensity
1.0
0.8
0.6
0.4
0.2
0.0
400
450
500
550
600
650
Wavelength (nm)

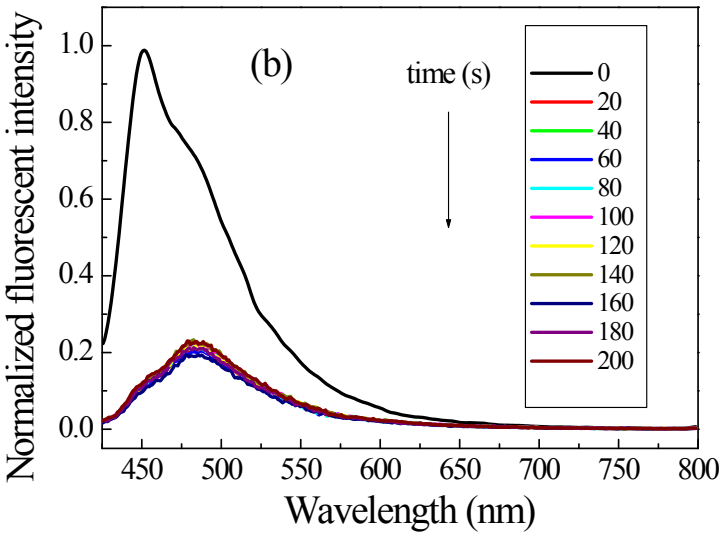
(b)
time (s)
0
20
40
60
80
100
120
140
160
180
200
Normalized fluorescent intensity
1.0
0.8
0.6
0.4
0.2
0.0
450
500
550
600
650
700
750
800
Wavelength (nm)

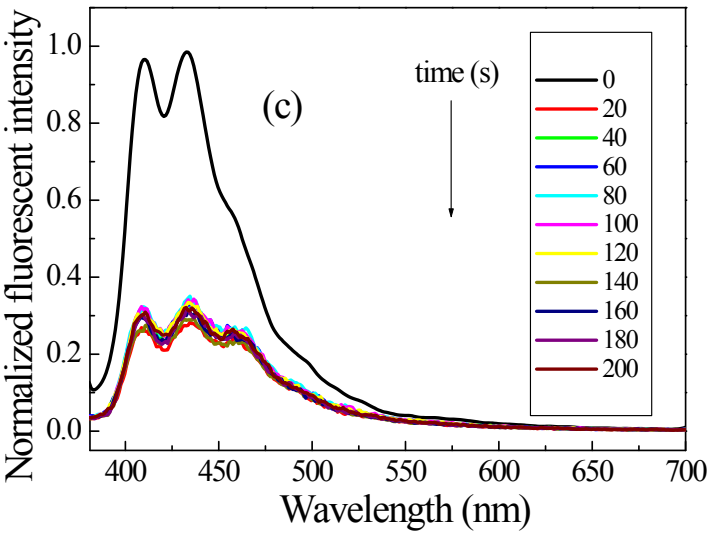
(c)
time (s)
0
20
40
60
80
100
120
140
160
180
200
Normalized fluorescent intensity
1.0
0.8
0.6
0.4
0.2
0.0
400
450
500
550
600
650
700
Wavelength (nm)

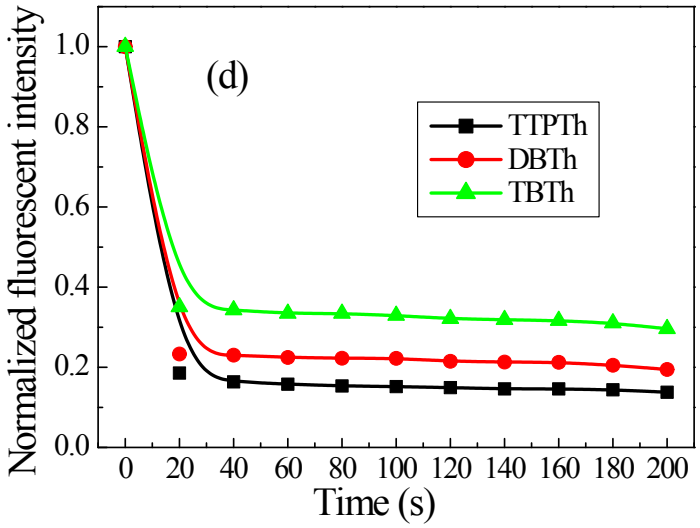

Fig. S10. Normalized fluorescence spectra of the CMPs dispersed solution upon addition of NACs. (a) TTPTh (DNP: 5.0×10^{-4} mol L^{-1}, in chloroform, λex=360 nm), (b) DBTh (DNP: 1.5×10^{-4} mol L^{-1}, in DMF, λex=410 nm), and (c) TBTh (DNP: 2.0×10^{-4} mol L^{-1}, in THF, λex=362 nm) for different periods of time. (d) Normalized fluorescence intensity of the CMPs dispersed solution upon addition of DNP.

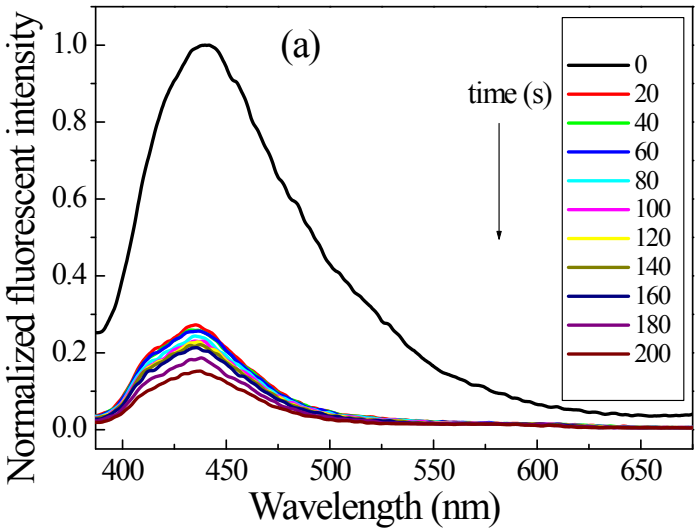
(a)
Normalized fluorescent intensity
Wavelength (nm)
time (s)
0
20
40
60
80
100
120
140
160
180
200

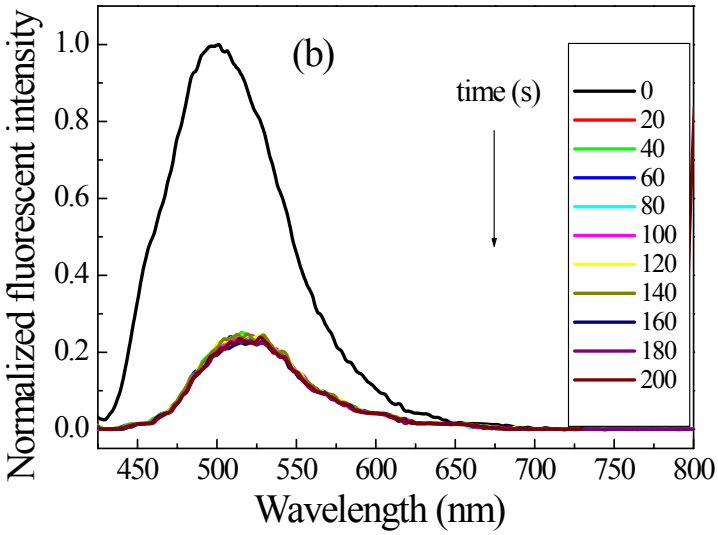
(b)
Normalized fluorescent intensity
Wavelength (nm)
time (s)
0
20
40
60
80
100
120
140
160
180
200

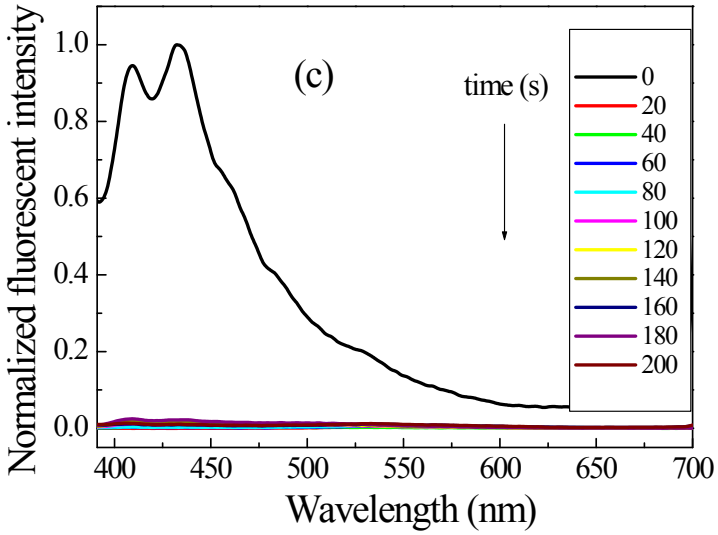
(c)
Normalized fluorescent intensity
Wavelength (nm)
time (s)
0
20
40
60
80
100
120
140
160
180
200

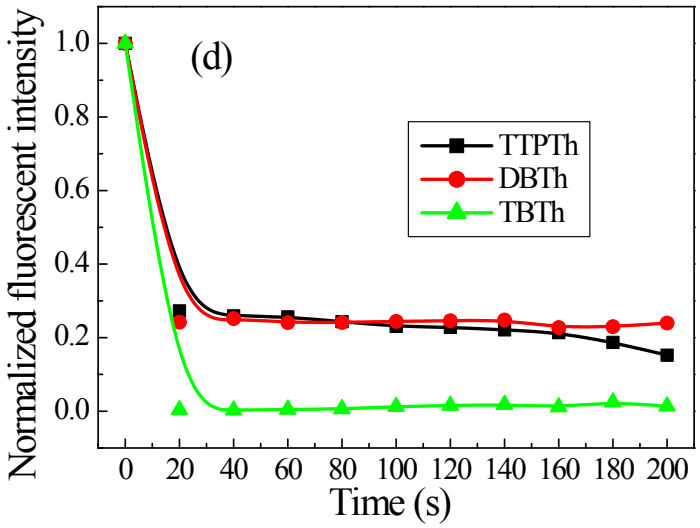

Fig. S11. Normalized fluorescence spectra of the CMPs dispersed solution upon addition of I_2. (a) TTPTh (I_2: 1.0×10^{-3} mol L^{-1}, in chloroform, λex=360 nm), (b) DBTh (I_2: 5.0×10^{-3} mol L^{-1}, in DMF, λex=410 nm), and (c) TBTh (I_2: 1.0×10^{-4} mol L^{-1}, in THF, λex=362 nm) for different periods of time. (d) Normalized fluorescence intensity of the CMPs dispersed solution upon addition of I_2.

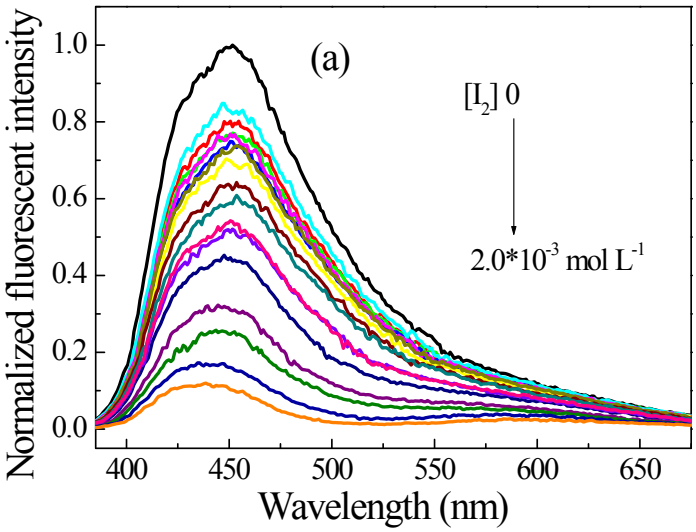
(a)
[I2] 0
2.0*10-3 mol L-1
Normalized fluorescent intensity
Wavelength (nm)
1.0
0.8
0.6
0.4
0.2
0.0
400
450
500
550
600
650

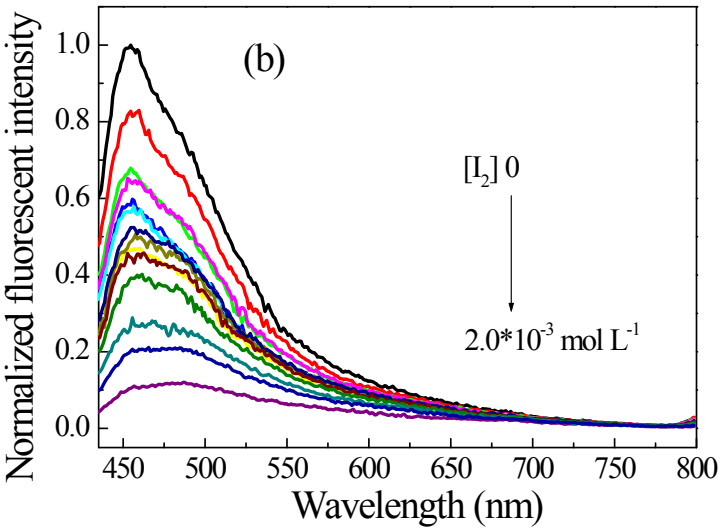
(b)
[I2] 0
2.0*10-3 mol L-1
Normalized fluorescent intensity
Wavelength (nm)
1.0
0.8
0.6
0.4
0.2
0.0
450
500
550
600
650
700
750
800

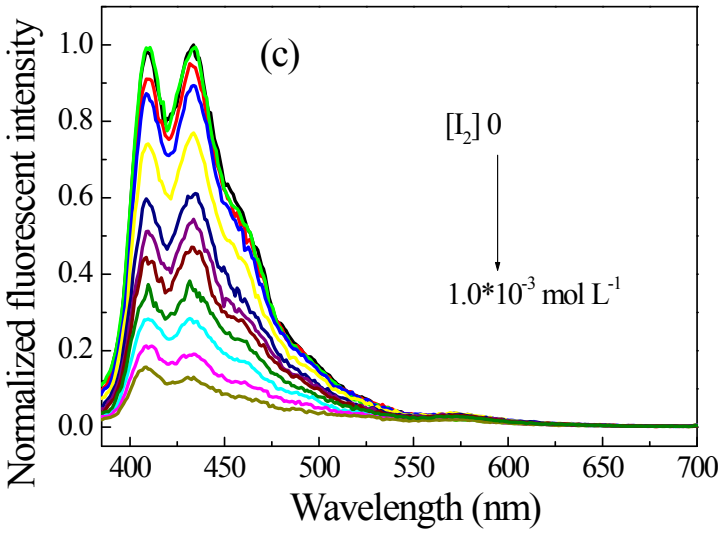
(c)
[I2] 0
1.0*10-3 mol L-1
Normalized fluorescent intensity
Wavelength (nm)
1.0
0.8
0.6
0.4
0.2
0.0
400
450
500
550
600
650
700

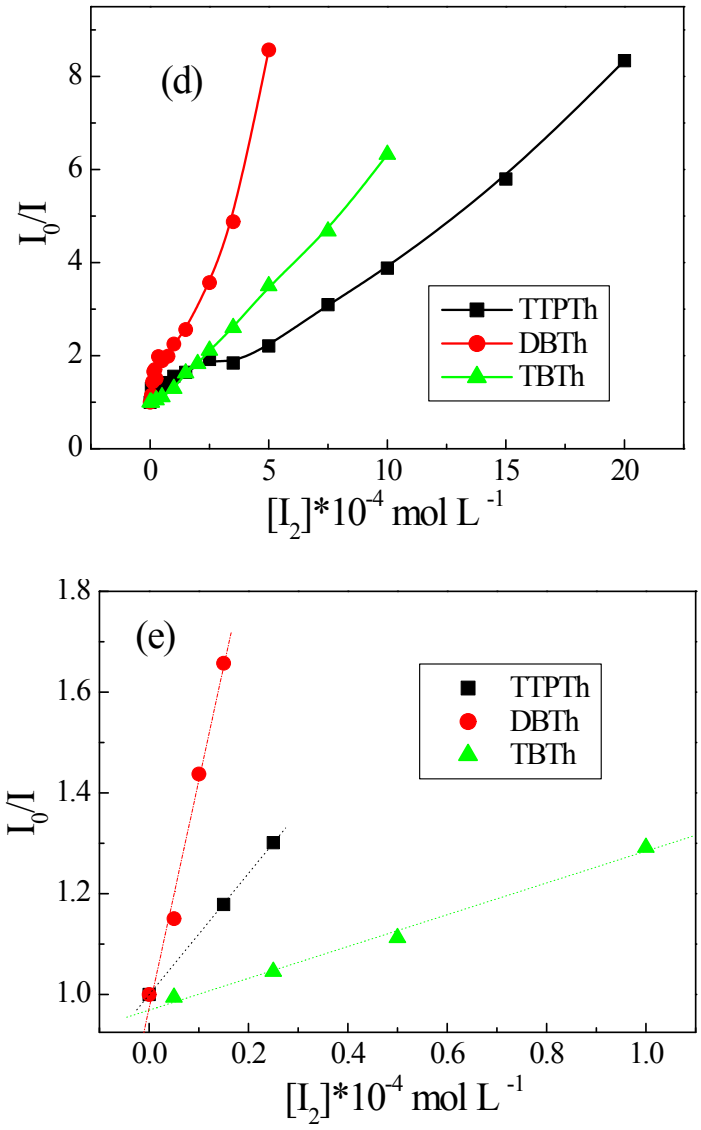

Fig. S12. The changes of fluorescent spectra of (a) TTPTh, (b) DBTh, and (c) TBTh in chloroform, DMF, and THF upon addition of I_2; (d) Relative fluorescence intensity (I_0/I) of the TTPTh, DBTh, and TBTh in suspensions upon addition of various concentrations of I_2; (f) Stern–Volmer plots of TTPTh, DBTh, and TBTh with various concentrations of I_2 (1.0 mg mL^{-1}, excited at 360, 410, and 362 nm).

Table S1. The equation of I_0/I of the CMPs to the concentrations of DNP or I_2 for suspension in chloroform (TTPTh), DMF (DBTh), and THF (TBTh).

CMPs	The equation	Regression coefficient (R)	The concentration range of NACs or I_2 (mol L^{-1})	detection limit (mol L^{-1})
TTPTh	$I_0/I=0.9913+1.10\times10^4[DNP]$	0.9974	0 to 1.0×10^{-4}	5.47×10^{-10}
DBTh	$I_0/I=1.0062+5.76\times10^4[DNP]$	0.9996	0 to 1.5×10^{-5}	1.56×10^{-10}
TBTh	$I_0/I=0.9502+9.59\times10^3[DNP]$	0.9991	5.0×10^{-6} to 1.0×10^{-4}	9.38×10^{-9}
TTPTh	$I_0/I=0.9972+1.20\times10^4[I_2]$	0.99997	0 to 2.5×10^{-5}	1.74×10^{-8}
DBTh	$I_0/I=0.9725+4.52\times10^4[I_2]$	0.9937	0 to 1.5×10^{-5}	3.32×10^{-12}
TBTh	$I_0/I=0.9691+3.15\times10^3[I_2]$	0.9965	5.0×10^{-6} to 1.0×10^{-4}	1.66×10^{-9}

Table S2. Summary of K_{sv} and LODs of thiophene-based CMPs for fluorescence sensing to NACs and iodine.

CMPs	Analyte	K_{sv} ($mol\ L^{-1}$)	detection limit ($mol\ L^{-1}$)	Refs
PTPATTh	PA	1.17×10^{3}(DOX)	6.39×10^{-8}	*Sensor. Actuat. B-Chem.* 2017, 244,
		5.00×10^{3}(THF)	3.01×10^{-9}	334–343.
TTPT	o-NP	6.20×10^{3}	2.18×10^{-9}	*Polym. Chem.* 2018, 9, 777–784.
PTThP-2	iodine	1.99×10^{3}	7.54×10^{-8}	*J. Polym. Res.* 2019, 26, 113–122.
PTThP-3		5.09×10^{3}	2.95×10^{-8}	
PTPTB	*p*-AP	7.08×10^{4}	4.2×10^{-6}	*Polym. Chem.* 2018, 9(27), *3832–*
				3839.
SNPs	NB	-	-	*Angew. Chem. Int. Edit.* 2018,
				57(43), 14188–14192.
SN-1	PA	2.78×10^{4}	-	*ACS Appl. Bio Mater. 2018, 1,*
SN-2	PA	1.31×10^{4}	-	*473−479.*
TTPTh	DNP	1.10×10^{4}	5.47×10^{-10}	*This work.*
DBTh	DNP	5.76×10^{4}	1.56×10^{-10}	
TBTh	DNP	9.59×10^{3}	9.38×10^{-9}	
TTPTh	iodine	1.20×10^{4}	1.74×10^{-8}	
DBTh	iodine	4.52×10^{4}	3.32×10^{-12}	
TBTh	iodine	3.15×10^{3}	1.66×10^{-9}	

p-AP—p-nitroaniline

Table S3. Summary of K_{sv} and LODs of other materials for determination of DNP.

materials	BET ($m^2\ g^{-1}$)	Methods or K_{sv} ($L\ mol^{-1}$)	detection limit ($mol\ L^{-1}$)	Refs
-	-	SPE and UHPLC –QTR AP® MS	1.85×10^{-10} (34 ng/l)	*Anal. Bioanal. Chem., 2013, 405, 5875–5885.*
SBA-15 CMK-3	660 1400	CMK-3-GC –MS method	1.09×10^{-8} (0.002 μg mL^{-1})	*Anal. Chim. Acta, 2011, 695, 58–62.*
GO-MIP/GCE composites	-	electrochemical sensor	4×10^{-7} (0.4 μM)	*Sensor. Actuat. B-Chem., 2012, 171–172, 1151–1158.*
SPE-MIPs	-	fluorescence detection	1×10^{-9} (1 nmol/L)	*Chinese Chem. Lett., 2014, 25, 1492–149.*
Dialysed caramel	-	fluorescence detection	1.4×10^{-7} (0.14μM)	*Talanta, 2019, 197, 159–167.*
MOFs	-	-	-	*J. Mater. Chem. A 2015, 3, 22369–22376.*
proximate pyrene units	-	fluorescence detection 1×10^{4}	-	*Tetrahedron Lett., 2015,56, 2311–2314.*
TTPTh	564.97	1.10×10^{4}	5.47×10^{-10}	*This work.*
DBTh	416.99	5.76×10^{4}	1.56×10^{-10}	
TBTh	521.30	9.59×10^{3}	9.38×10^{-9}	

Table S4. Summary of K_{sv} and LODs of POPs for fluorescence sensing to iodine

Sample	BET ($m^2 g^{-1}$)	K_{sv} ($L mol^{-1}$)	LOD ($mol L^{-1}$)	Refs
TTPA	308	2.38×10^4	3.22×10^{-11}	*Micropor. Mesopor. Mat. 2019,*
TTDATA	491	4.33×10^2	-	*273, 163–170*
TTMDATA	456	7.31×10^2	-	
TS-TAD	828,	5.76×10^3	1.56×10^{-9}	*Eur. Polym. J. 2019,*
TS-TADP	783	5.59×10^3	8.05×10^{-11}	*115, 37–44*
Cz-TPM	713.2	2372(I^-)	-	*ACS Appl. Mater. Interfaces*
				2017, 9 (25), 21438–21446
PTThP-2,	370.8	1.99×10^3	7.54×10^{-8}	*J. Polym. Res.* 2019, 26, *113–*
PTThP-3	748.2	5.09×10^3	2.95×10^{-8}	*122.*
TTTAT	564.8	1.53×10^5	2.98×10^{-12},	*Micropor. Mesopor. Mat. 2019,*
TTDAT	44.1	9.07×10^4	2.96×10^{-13}	*284, 468–475.*
TDPA	56.52	1.85×10^4	1.62×10^{-11}	*J. Appl. Polym. Sci.*
TTPBTA	2.486	6.56×10^4	6.86×10^{-12}	*2019, 49255.*
TDPDB	592.18	5.83×10^4	2.57×10^{-12}	*Polym. Adv. Technol. 2020,*
				31(6), 1388-1394.
TDP	261.9	6.10×10^4	3.14×10^{-13}	*New J. Chem., 2020, 44, 2312-*
PCPP	43.0	1.40×10^5	2.46×10^{-12}	*2320.*
TTPDP	187.5	2.02×10^4	2.25×10^{-12}	
TDTPAP	695.2	4.65×10^3	3.25×10^{-10}	
TDTPAPz	561.3	3.76×10^3	2.47×10^{-11}	*Environ. Sci. Pollut. Res.*
TTDPz	13.5	1.10×10^3	1.36×10^{-10}	*27(16), 20235-20245.*
TBIM	8.12	1.16×10^4	1.29×10^{-10}	*J. Mater. Chem. A, 2020, 8,*
				2820–2826.
TTPTh	564.97	1.20×10^4	1.74×10^{-8}	*This work.*
DBTh	416.99	4.52×10^4	3.32×10^{-12}	
TBTh	521.30	3.15×10^3	1.66×10^{-9}	

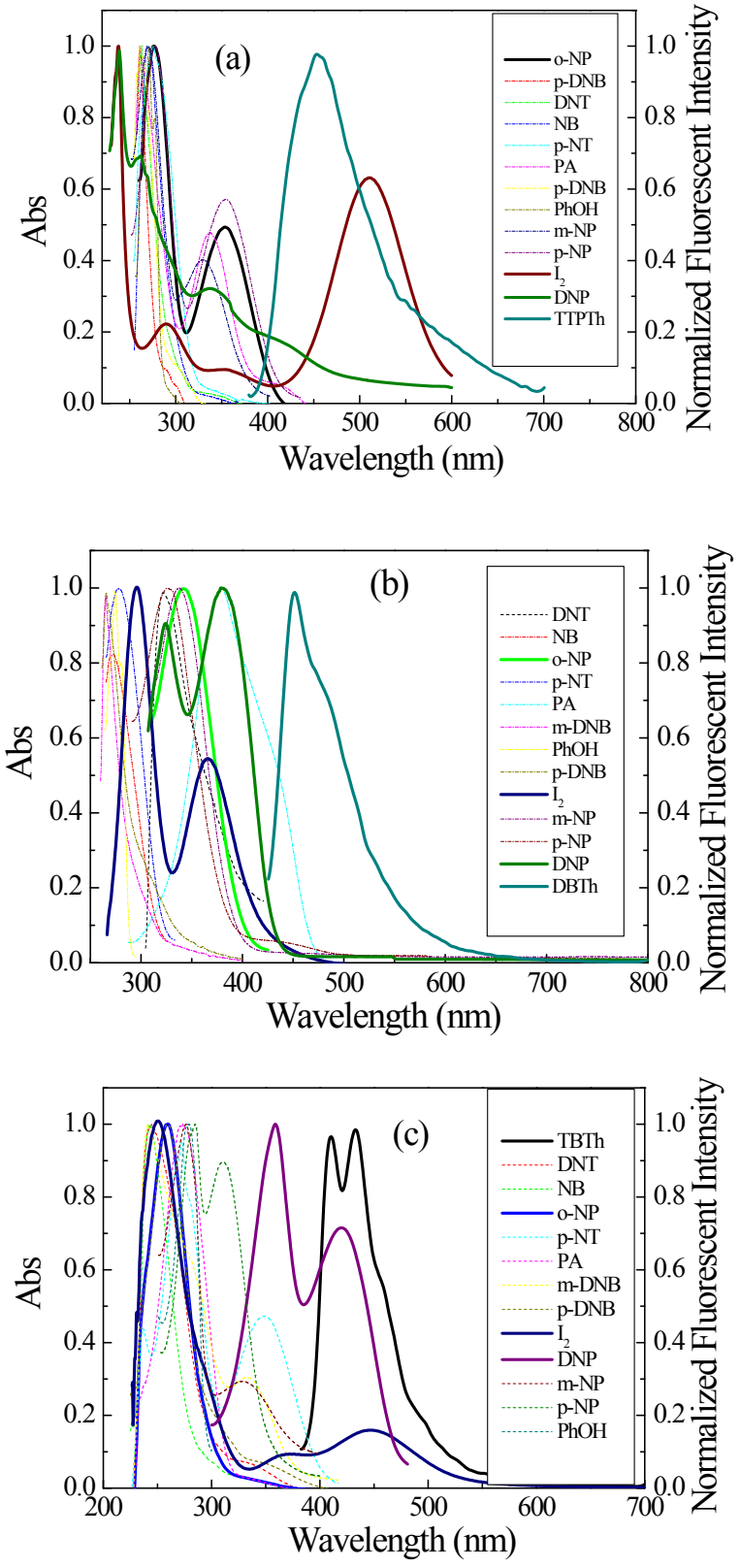

Fig. S13. Normalized absorption spectra of analytes and emission spectra of (a) TTPTh in chloroform (excitation wavelength: 360 nm), (b) DBTh in DMF (excitation wavelength: 410 nm), and (c) TBTh in THF (excitation wavelength: 362 nm).

Table S5. HOMO and LUMO calculations for CMPs, NACs and I_2. All the molecular orbital calculations were performed with the Gaussian 09 D.01 program at the B3LYP/6-31G* level.

MO energy (eV)	TTPTh	DBTh	TBTh	I_2	PA
LUMO	-1.726	-1.255	-2.063	-4.988	-3.898
HOMO	-5.424	-6.128	-5.628	-7.553	-8.273
MO energy (eV)	DNP	o-NP	m-NP	p-NP	NB
LUMO	-3.320	-2.711	-2.396	-2.222	-2.428
HOMO	-7.628	-6.797	-6.779	-6.721	-7.591
MO energy (eV)	m-DNB	p-DNB	DNT	p-NT	PhOH
LUMO	-3.135	-3.495	-2.977	-2.318	-0.3331
HOMO	-8.413	-8.358	-8.113	-7.364	-6.566

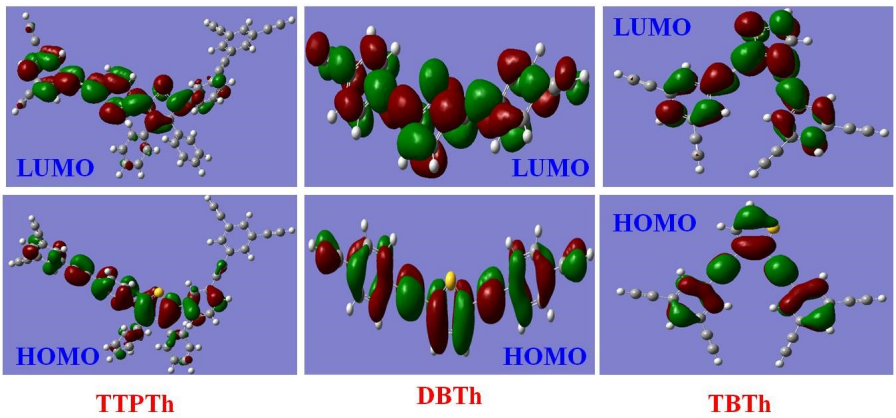

Fig. S14. HOMO and LUMO orbital diagrams of CMPs. The molecular orbital calculations were performed with the Gaussian 09 D.01 program at the B3LYP/6-31G (d) level.

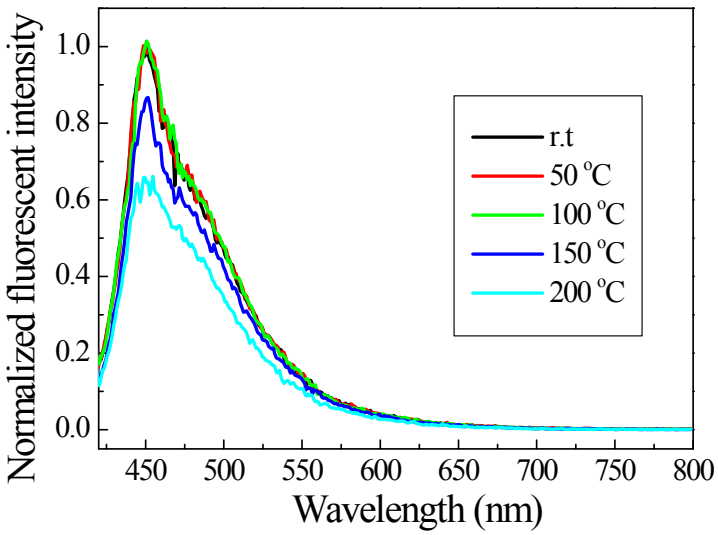

Fig. S15. Fluorescent spectra of DBTh before and after annealing at different temperatures for 30 min in air.

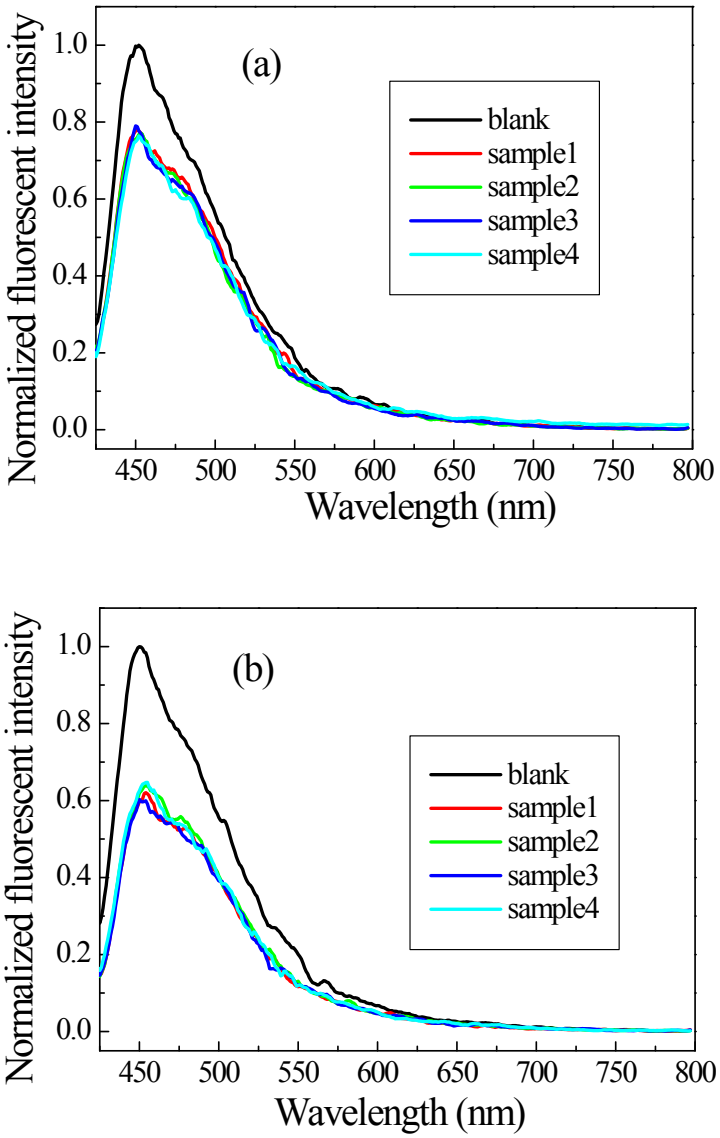

Fig. S16. The practical application of DBTh as a chemosensor for DNP in sand samples. The addition of DNP (μmol/5g): (a) 0.125, (b) 0.250.

Table S6. Spiked recoveries and RSDs (%, n=4) for the determination of DNP in sand samples using the DBTh sensor.

Added (μmol /5g)	Added ($\times10^{-6}$ mol L^{-1})	Found ($\times10^{-6}$ mol L^{-1})	Found (μmol /5g)	Recovery ±RSD (%)
0.125	5.0	5.10	0.127	0.122±4.28
0.125	5.0	4.70	0.117	
0.125	5.0	5.045	0.126	
0.125	5.0	4.74	0.118	
Added (μmol /5g)	Added ($\times10^{-6}$ mol L^{-1})	Found ($\times10^{-6}$ mol L^{-1})	Found (μmol /5g)	Recovery ±RSD (%)
0.250	10.0	10.512	0.263	0.246±3.85
0.250	10.0	9.693	0.242	
0.250	10.0	11.326	0.283	
0.250	10.0	9.349	0.234	

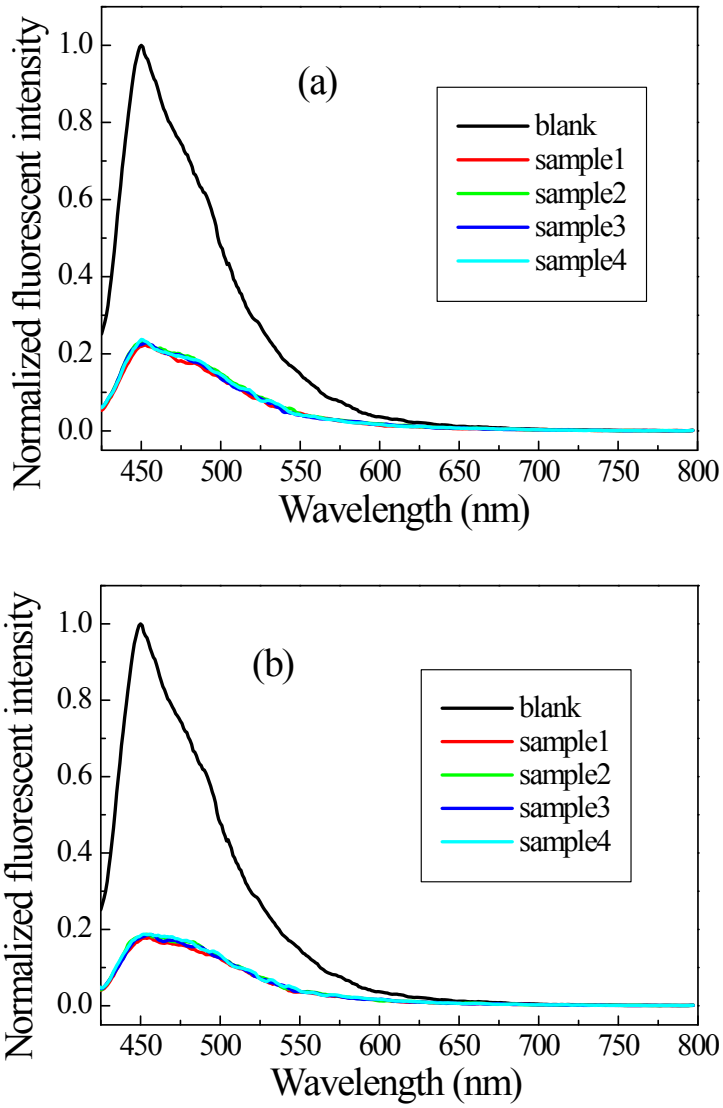

Fig. S17. The practical application of DBTh as a chemosensor for I_2 in sand samples. The addition of I_2 (μmol/5g): (a) 0.025, (b) 0.050.

Table S7. Spiked recoveries and RSDs (%, n=4) for the determination of I_2 in sand samples using a DBTh sensor.

Added (μmol /5g)	Added ($\times 10^{-6}$ mol L^{-1})	Found ($\times 10^{-6}$ mol L^{-1})	Found (μmol /5g)	Recovery ±RSD (%)
0.025	1.0	0.852	0.0213	0.0234±3.94
0.025	1.0	0.954	0.0238	
0.025	1.0	1.082	0.0271	
0.025	1.0	0.863	0.0216	
Added (μmol /5g)	Added ($\times 10^{-6}$ mol L^{-1})	Found ($\times 10^{-6}$ mol L^{-1})	Found (μmol /5g)	Recovery ±RSD (%)
0.050	2.0	1.619	0.0405	0.0468±3.53
0.050	2.0	1.387	0.0347	
0.050	2.0	1.994	0.0498	
0.050	2.0	1.949	0.0487	